Copyright

IEEE Catalog Number: CFP09ECD-CDR
ISBN: 978-1-4244-2893-9
LOC: 2008935511

Omnipress
2600 Anderson St
Madison, WI 53704
1-800-828-0305

For technical support click here

Monday, September 21, 2009
10:45AM-12:00PM

Session S2-1: Inverter Control
SECOND LEVEL, CEDAR
Chair: P. Zanchetta, University of Nottingham, UK

10:45AM **Predictive Current Control of Grid-Connected DC-AC Converters During Network Unbalance**
Jiabing Hu, Yikang He, Heng Nian and Hongsheng Wang
Zhejiang University, China

11:10AM **Flux Estimation Techniques for Inrush Current Mitigation of Line Interactive UPS systems**
Yu-Hsing Chen and Po-Tai Cheng
National Tsing Hua University, Taiwan

11:35AM **A Hybrid Control Method for Three-Phase Grid-Connected Inverters with High Quality Power**
Zitao Wang and Liuchen Chang
University of New Brunswick, Canada

Session S2-2: dc-dc Converter Topologies
SECOND LEVEL, PINE
Chair: W. Peterson, E&M Power, USA

10:45AM **Comparison of Two Different Cell Topologies for a Multilevel Power Supply to achieve High Efficiency Envelope Amplifier**
Daniel Diaz, Miroslav Vasic, Pedro Alou, Oscar Garcia, Jesus A. Oliver, and Jose A. Cobos
Universidad Politecnica de Madrid, Spain

11:10AM **Three Level Buck Converter with Control and Startup**
David Reusch, Ming Xu and Fred C. Lee
Virginia Tech, United States

11:35AM **Digitally Controlled Distributed Multiphase DC-DC Converters**
Xu Zhang, Luca Corradini and Dragan Maksimovic
University of Colorado at Boulder, United States

Session S2-3: Inverters for Solar Energy Systems
LOWER LEVEL, SAN JOSE/SANTA CLARA
Chair: Y-S Suh, Chonbuk National University, South Korea

10:45AM **Modeling and Control of the Single-Phase Photovoltaic Grid-Connected Cascaded H-Bridge Multilevel Inverter**
S. J. Lee, H. S. Bae and Bo Hyung Cho
Seoul National University, Korea (South)

11:10AM **New MPPT Algorithm for Photovoltaic Systems Connected to NPC Converters**
Manuel Galvez, Emilio Bueno, Francisco J. Rodriguez, Francisco J. Meca and Ana Rodriguez
Alcala University, Spain; University of Alcala, Spain

11:35AM **A Single Phase Curren Source Solar Inverter with Reduced DC Link and Improved Maximum Power Point Tracking**
Craig Bush and Bingsen Wang
Arizona State University, United States

Session S2-4: dc-dc Converters for Distributed Generation Systems
LOWER LEVEL, CARMEL/MONTEREY
Chair: B. Ozpineci, Oak Ridge National Laboratory, USA

Session S2-5: Inverter PWM and Control Techniques
LOWER LEVEL, SAN MARTIN/SAN SIMEON
Chair: K. Matsuse, Meiji University, Japan

10:45AM **Dead-Time Elimination Method and Current Polarity Detection Circuit without Separate Power Sources for Three-Phase Inverter**
Yong-Kai Lin and Yen-Shin Lai
National Taipei University of Technology, Taiwan

11:10AM **Enhanced Three Phase AC Stationary Frame PI Current Regulators**
Wang Y. Kong, D. Grahame Holmes and Brendan P. McGrath
Monash University, Australia

11:35AM **Asymmetric Interleaving - A New Approach to Operating Parallel Converters**
Troy Beechner and Jian Sun
Rensselaer Polytechnic Institute, United States

Session S2-6: Wide-Bandgap Semiconductors and Applications
LOWER LEVEL, SAN CARLOS/SAN JUAN
Chair: E. Santi, University of South Carolina, USA

10:45AM **Roadmap for Megawatt Class Power Switch Modules Utilizing Large Area Silicon Carbide MOSFETs and JBS Diodes**
Jim Richmond, Scott Leslie, Brett Hull, Mrinal Das, Anant Agarwal and John Palmour
Cree Inc., United States; Powerex Inc, United States

11:10AM **20 A, 1200 V 4H-SiC DMOSFETs for Power Conversion Systems**
Brett Hull, Mrinal Das, Fatima Husna, Robert Callanan, Anant Agarwal, and John Palmour

11:35AM **Investigation on Inherently Safe Gate Drive Techniques for Normally-On Wide Bandgap Power Semiconductor Switching Devices**
Mi Dong, John Elmes, Michael Pepper, Issa Batarseh and Z. John Shen
University of Central Florida, United States

Session S2-7: PM Machines: Design, Analysis, and Optimization
SECOND LEVEL, FIR
Chair: D. Ionel, AO Smith, USA

10:45AM **Analysis of Slanted Air-gap Structure of Interior Permanent Magnet Synchronous Motor with Brushless Field Excitation**
Seong T. Lee and Leon Tolbert
The University of Tennessee, United States; Oak Ridge National Laboratory, United States

11:10AM **Torque Ripple Reduction of Axial Flux Permanent Magnet Synchronous Machines with Segmented and Laminated Stator**
Weizhong Fei and Patrick Luk
Cranfield University, United Kingdom

11:35AM **Rotor Saliency Improved Structural Design For Cost Reduction in Single-phase Line-Start Permanent Magnet Motor**
Liang Fang, Byeong-Hwa Lee, Jung-Pyo Hong and Hyuk Nam
Hanyang University, Korea (South); IG Electronics Inc., Korea (South)

Session S2-8: Induction Motor Drives
SECOND LEVEL, OAK
Chair: G. Capolino, University of Picardie, France

10:45AM **Flux Weakening Strategy of an Induction Machine Driven by an Electrolytic Capacitor-less Inverter**
Anno Yoo, Seung-Ki Sul, Sunja Kim and Kyung-Seo Kim
Seoul National University, Korea (South); LS Industrial System Co., Korea (South)

Rotor Saliency Improved Structural Design For Cost Reduction in Single-phase Line-Start Permanent Magnet Motor

Liang Fang, B. H. Lee, Jung-Pyo Hong*
*Senior Member, IEEE
Hanyang University
17 Haengdang-dong, Seongdong-gu
Seoul 133-791, Korea
fangliangicw@hotmail.com, hongjp@hanyang.ac.kr

Hyuk Nam
LG Electronics Inc.
Changwon 641-711, Korea
hnam@lge.com

***Abstract* -- This paper presents a study on motor material cost reduction by emphasizing rotor structural advantage in machine performance promotion of a single-phase line-start permanent magnet motor (LSPMM). The cost reduction of LSPMM is focused on saving high-price PM material in the LSPMM design. In the paper, a double-layer interior-PM (IPM) rotor structure is finally adopted to create higher rotor saliency ratio for improving reluctance torque generation to compensate decreased magnet torque due to PM usage reduction. That is, the hybrid torque with higher balance ratio of reluctance toque to magnet torque helps to lower the dependency o PM materials usage. With given torque and efficiency constrains, a series of double-layer rotor structures are built and optimized with gradually reduced amount of PM material. The torque and efficiency performances of LSPMM are predicted by using equivalent circuit method coupled with finite element analysis (FEA). The computed motor torque and efficiency performances are confirmed by comparing with test results.**

***Index Terms*—Cost reduction, double-layer IPM design, FEA, hybrid torque, LSPMM, torque and efficiency constrains.**

I. INTRODUCTION

The single-phase induction motors (IM) are well known as their simplicity, rugged construction and relative lower manufacturing cost, especially the line-start capability that being fed directly from the commercial single-phase voltage source without any type of control device [1]. However, their relative low efficiency performance can not satisfy the increasing demand of high-efficiency and energy-saving in an industrial point of view recently. On the other hand, the interior permanent magnet synchronous motors (IPMSM) are attractive for their high efficiency and high torque density, but the IPMSM requiring an expensive inverter for operation [2]. Therefore, line-start PM motor (LSPMM) is being developed as a high-efficiency alternative to the induction motor [1].

The LSPMM has PM segments and inner air-gap regions buried into the caged rotor of IM, thus it can generate asynchronous starting torque by means of induction caged rotor, and utilizing hybrid torque at synchronously running, which guarantees high efficiency at steady state operation [2]. In general, the LSPMM has beneficial attributes of both IM and IPMSM, are excellent candidate for household applications, such as compressors of air-condition and refrigerator, which has the largest portion of power used [3].

However, these performance advantages are always negated by high cost of PM material. Although the price of PM is gradually decreasing, the reduction of magnet usage in PM machine design is always an important objective. Therefore, an efficient approach for guiding PM usage reduction in IPM machine design is very expected, but few papers focused on it. This paper presents a study on PM cost reduction by decreasing PM material usage in a double-layer design LSPMM. It is developed from an IM for improving torque and efficiency performance. Similar to the IPM rotor design, the characteristics of LSPMM are quite sensitive to the rotor inner structure. For generally concluding the PM reduction approach, the rotor structure is optimized with few design variables and in a certain design process.

From machine performance standpoint, the buried PM in LSPMM helps to improve steady state performance, but also prevents the self-starting operation since the magnet braking torque weaken the induced starting torque due to cage bars [4]. This study adopts reducing PM and emphasizing the advantages of multi-layer IPM rotor structure in motor torque and efficiency improvement, the deteriorated machine performances caused by reducing PM usage is compensated by employing higher saliency rotor structure. The higher rotor saliency, the lesser magnet material is necessary in IPM motor for maintaining the same machine performance [2]. Since the higher-saliency usually relates to more complex rotor structure design, the tradeoff of PM material cost reduction and manufacture difficulties must be considered.

The LSPMM torque and efficiency performance are predicted by using equivalent circuit method (ECM) coupled with finite element analysis (FEA) for machine parameter calculation. In final, the LSPMM is test, and a general good agreement confirmed the present performance analysis.

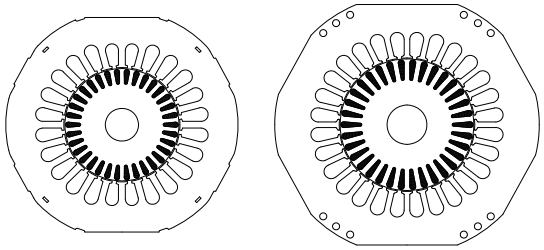

(a) IM_a @Power 1000W (b) IM_b @Power 2000W
Fig. 1. Configuration of base IM analysis models

II. Model and Analysis Method

In this study, two existing single-phase capacitor-run 1000W/2000W induction motors used as air-condition compressors are firstly introduced as basic models. Fig. 1 shows their cross sections. TABLE I compares their tested performances, that stating torque, maximum output torque capability and efficiency at rated operation are emphasized.

For improving machine efficiency, the two IMs are developed to be LSPMMs by implanting PM segments into caged rotor. In Fig. 2, a basic LSPMM model adopting popular double-layer IPM rotor structure design is illustrates. The prospective improvements, as well as constrains of machine performance in LSPMM designs are given as TABLE I lists.

The IM stator structure is maintained and the main and auxiliary windings connection is illustrated as the electric circuit shows in Fig. 3. The starting capacitances (C_s), running capacitances (C_r) and positive temperature coefficient (PTC) are connected to auxiliary winding in parallel for increasing starting torque and power factor [4].

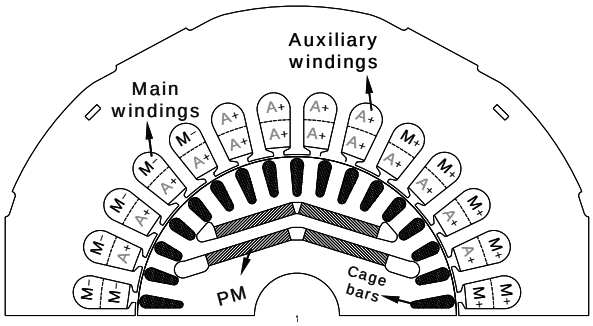

Fig. 2. Single-phase LSPMM model with double-layer IPM rotor design

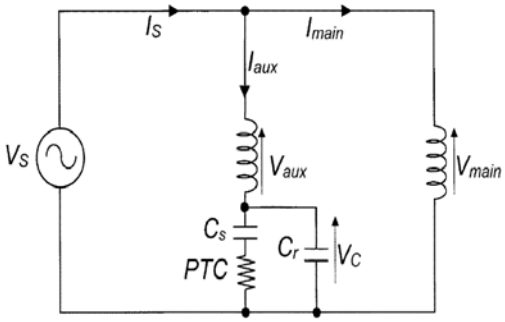

Fig. 3. Single-phase line-start LSPMM stator windings circuit

TABLE I
PERFORMANCES OF BASE INDUCTION MOTORS BY TEST

Items	Unit	Base IM_a	Base IM_b	LSPMM
Output Power	[W]	1000	2000	Keep
Start Torque	[Nm]	1.10	2.10	Improve
Max. Torque	[Nm]	6.4	13.3	Keep
Ave. Torque	[Nm]	3.1	6.65	Keep
Efficiency	[%]	86.11	86.9	+3.0 [%]
Power factor	[%]	67.2	68.8	Improve

A. LSPMM Performance Analysis

In this study, the single-phase LSPMM design is examined focusing on the asynchronous start-up performance and synchronous running operation at steady state. For efficiently analyzing the motor characteristics, a well recognized efficient equivalent circuit method established by T.J.E. Miller is used in the study.

1. Starting Torque Characteristic

During asynchronous start-up operation, the starting torque of LSPMM is mainly considered by the average cage torque (T_cage) and the magnet braking torque (T_mag) [5], as Fig. 4(a) illustrates. The T_cage is inducted by rotor cage-bars as "IM action", and the T_mag is produced due to the reaction of currents induced from the magnet flux in stator windings [4]. Fig. 4(b) separately shows the variation of feeding currents in main and auxiliary windings corresponding to the asynchronous starting variation.

By utilizing the equivalent circuit proposed by T.J.E. Miller [4], the starting torque is analyzed with the variation of main/auxiliary windings ratio, cross section of cage bars, and assistant capacitors C_s and C_r, as Fig. 5 illustrate. The proper values for generating required starting torque in the LSPMM design can be easily chosen. Compare with the base IM, the developed LSPMM usually need larger starting capacitor C_s or/and running capacitor C_r for generates enough starting torque in asynchronous start-up operation.

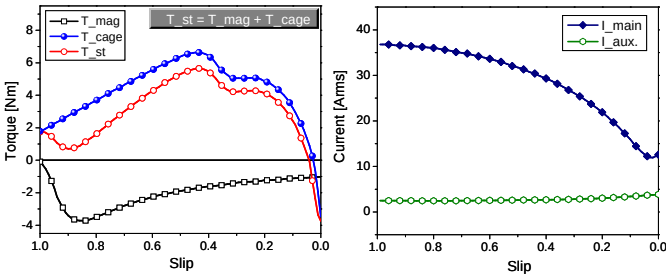

(a) Starting torque generation (b) Currents in main/auxiliary windings
Fig. 4. LSPMM start-up performance analysis using ECM

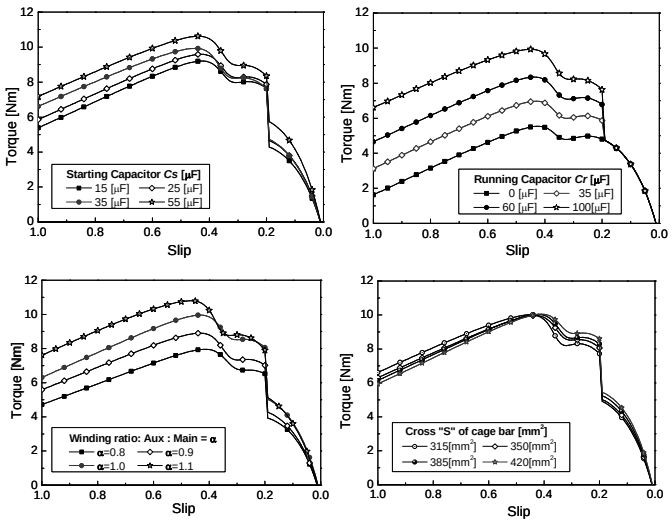

Fig. 5. LSPMM asynchronous starting torque examined by ECM

2. *Steady-State Performance Analysis*

The steady state performances of LSPMM at synchronous running operation are analyzed by equivalent circuit method coupled with finite element analysis based on coordinate transformation.

In theory, the single-phase LSPMM can be converted into a two-phase frame of *d-q* plane, and then the unbalanced field is dealt with symmetrical coordinate method [3]. Fig. 6 shows the vector diagram in *d-q* plane. The LSPMM performances are calculated by carrying out following equivalent circuits, that composed of *d*-axis/*q*-axis positive sequence circuits and negative sequence circuit respectively, as Fig. 7 gives. The appearing circuit parameters are precisely calculated by FEA, such as the fundamental component of phase back-EMF, *d-q* axis inductances varying with currents and phase angles, and iron losses.

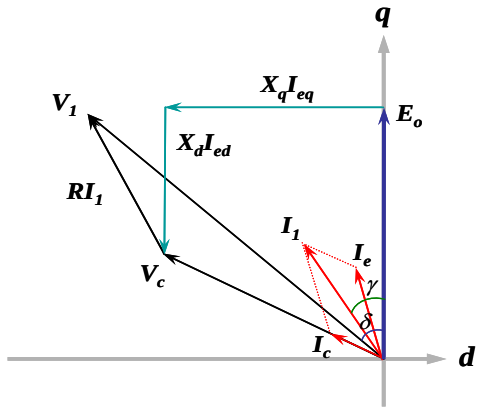

Fig. 6. Vector diagram of single-phase LSPMM in *d-q* plane

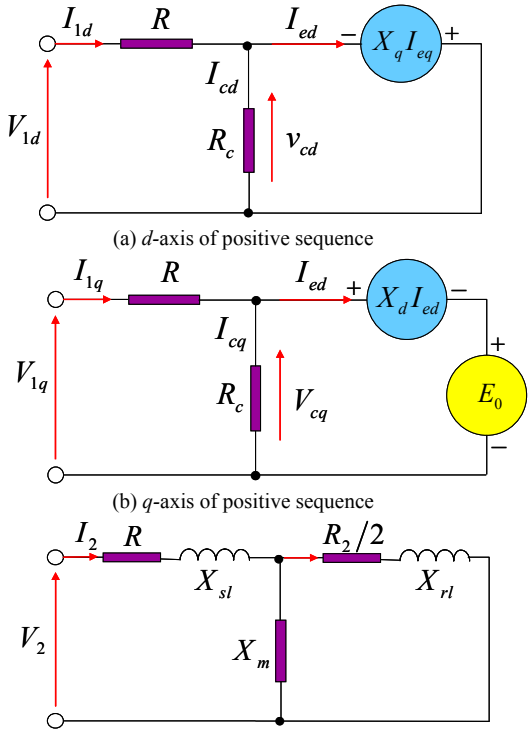

(a) *d*-axis of positive sequence

(b) *q*-axis of positive sequence

(c) Negative sequence

Fig. 7. Steady state equivalent circuits of single-phase LSPMM

The steady state performances of LSPMM are similar to IPMSM, that hybrid synchronous torque is generated at synchronous operation. According to the presented vector diagram and *d-q* axis equivalent circuits, as well as the stator electric circuit, the voltage and current equations, and output power, torque production, motor efficiency performance calculation are given as following equations [6], [7]:

$$\begin{cases} I_{1d} = I_{ed} + I_{cd} \\ I_{1q} = I_{ed} + I_{cq} \end{cases} \quad [1]$$

$$\begin{cases} V_{1d} = RI_{1d} - X_q I_{eq} \\ V_{1q} = RI_{1q} + X_d I_{ed} + E_o \end{cases} \quad [2]$$

$$\begin{cases} \mathrm{I}_{\mathrm{aux}} = \dfrac{1}{\sqrt{2}}\left[\mathrm{I}_1\left(1 + j\dfrac{\cot\varepsilon}{\beta}\right) + \mathrm{I}_2\left(1 - j\dfrac{\cot\varepsilon}{\beta}\right)\right] \\ \mathrm{I}_{\mathrm{main}} = -\dfrac{1}{\sqrt{2}\beta}\csc\varepsilon\left[\mathrm{I}_1 - \mathrm{I}_2\right] \end{cases} \quad [3]$$

$$\begin{cases} P_{out} = P_1 + P_2 = \left(\mathrm{Re}(\mathrm{V}_1\mathrm{I}_1^*) - RI_1^2\right) - \left(\mathrm{Re}(\mathrm{V}_2\mathrm{I}_2^*) - RI_2^2\right) \\ \eta_{eff} = \dfrac{\mathrm{V_S}\cdot\mathrm{I_S}}{P_{out}} \times 100\% \end{cases} \quad [4]$$

$$\begin{cases} T = T_{Ps} + T_{Ns} = P_1/\omega_s + P_2/\omega_s \\ {}^{*}T_{Ps} = \left(T_M + T_R\right) = p\left(E_o I_{1q} + (L_d - L_q) I_{1d} I_{1q}\right) \end{cases} \quad [5]$$

where, I_e is effective current in the positive sequence circuit, I_c is current consumed in iron loss, R_a is equivalent phase winding resistance, R_c is equivalent iron loss resistance, β is effective turn ratio between the main/auxiliary windings, ε is electrical angle between d-q axis, E_o is no-load back-EMF.

III. Magnet Reduction and Rotor Structure Design

The LSPMM utilizes hybrid torque at synchronous operation, as the above torque equation presented. In this paper, the magnet reduction is realized by improving the hybrid torque characteristic, that increasing reluctance torque to compensate magnet torque, which helps to lower the dependency on magnet usage in LSPMM [8].

A. Balance of Hybrid Torque Components

The hybrid torque production is considered as reluctance torque adding to magnet torque spatially [2]. Therefore the same maximum hybrid torque (T_{Hy}) is possible to be generated with different balance ratio (γ) of reluctance torque (T_R) to magnet torque (T_M), for example γ_a=(3:10) and γ_b=(6:7), as Fig. 8 (a), (b) show. The higher balance ratio usually relates to high rotor saliency characteristic, which is defined in term of d-q axis inductance, as (L_q/L_d).

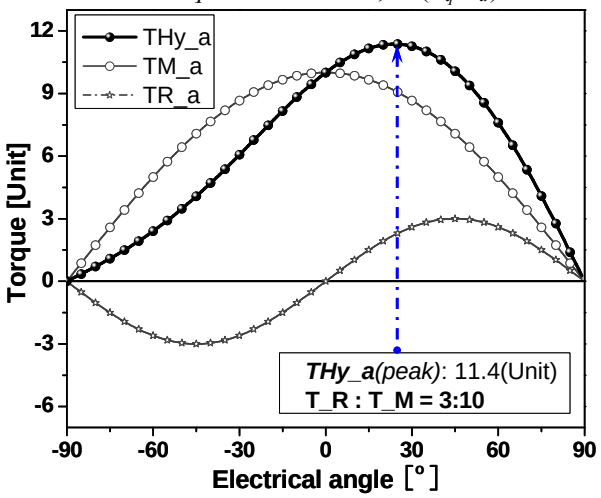

(a) Identical hybrid torque $T_{\_peak}$ with low ratio of (T_R/T_M)

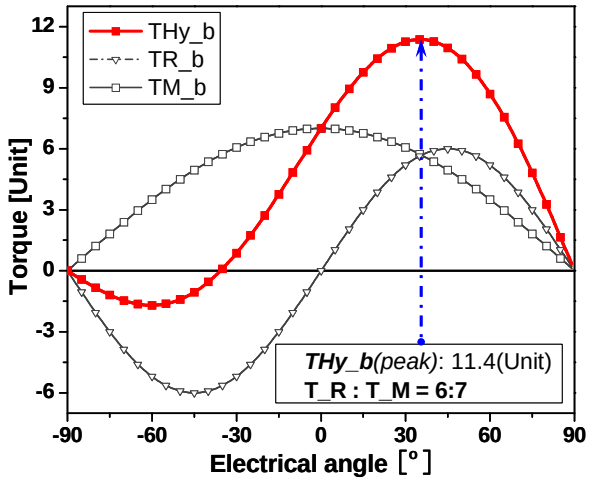

(b) Identical hybrid torque $T_{\_peak}$ with high ratio of (T_R/T_M)

Fig. 8. Hybrid torque characteristics according to different balance ratio

B. Multi-Layer IPM Design and Rotor Saliency Effect

For satisfying the torque and efficiency constrains in magnet reduction design, the geometry of IPM rotor structure is optimized to create higher rotor saliency. The higher rotor saliency benefits to reluctance torque T_R generation, which can be used to compensate the decreased magnet torque T_M production since less permanent magnet employed in IPM rotor design for generating specific torque.

The rotor saliency is created since the high reluctance exists along d-axis due to the low permeability of buried PM and air-gap regions, while along q-axis between magnet poles, exists no magnetic barriers, the reluctivity to magnetic flux is very low [2]. As the rotor saliency definition in term of d-q axis inductances, the rotor saliency improvement is desired by enlarging the difference of d-axis and q-axis inductances. However, the decrease of d-axis inductance is different without increasing magnet usage, even though the buried air-gap regions can be utilized at a certain extend. On the other hand, the increase of q-axis inductance is also limited due to the enlarged flux-barriers regions and magnetic saturation [2].

In this part, based on the single-phase 1000W IM_a, a series LSPMM models are designed with splitting constant PM material to create multi-layer IPM structure for enhancing rotor saliency effect. The torque and efficiency performances of LSPMMs are compared with IM_a for analysis of rotor structure advantage in machine performance.

As Fig. 9 illustrates, the base IM_a model is developed to three optimized LSPMM models, including two double-layer design models (2-segment PM per pole design and 4-segment PM per pole design) and a triple-layer design model. Obviously, the difficulty and manufacture cost is gradually increased even justifying from the rotor structure.

The comparison of machine performances are generally well confirmed by tested, as TABLE II lists. It reveals that multi-layer IPM rotor design benefit to torque and efficiency improvement due to the enhanced rotor saliency. But also, it

will unavoidably cause mechanical robustness and high manufacture difficulty problem in practice, even running a risk of irreversible demagnetization in the thin PM segments. For a tradeoff of performance improvement and low-cost simplicity manufacture, the double-layer IPM rotor design of 4-segment PM per pole structure, marked as model "M2b", is chosen for the magnet reduction analysis depending on rotor geometry optimization in next section.

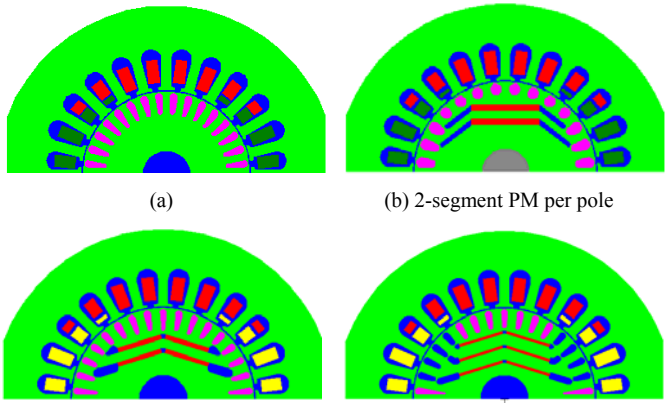

(a) (b) 2-segment PM per pole

(c) 4-segment PM per pole (d) 6-segment PM per pole

Fig. 9. Multi-layer LSPMM design based on IM_a with same PM material: (a) Basic IM_a model; (b) Double-layer IPM design, M2A; (c) Double-layer IPM design, M2B; (d) Triple-layer LSPMM design M3

TABLE II
PERFORMANCE COMPARSION IN MULTI-LAYER ROTOR DESIGN

Model	IM_a (test)		M_2A	M_2B (test)		M_3
PM usage [g]	0		120	120		120
Saliency	-		2.3	2.8		3.0
I_LL. [Arms]	5.00	(5.56)	6.11	5.08	(5.65)	5.75
T_Max. [Nm]	6.42	(7.55)	6.92	6.76	(7.46)	7.69
T_Ave. [Nm]	3.1	(3.1)	3.07	3.09	(3.09)	3.09
Efficiency [%]	89.38	(86.11)	90.61	92.20	(89.71)	92.27
Total Cost	100		152	155		160
Robust	Good		Safe	Safe		Weak

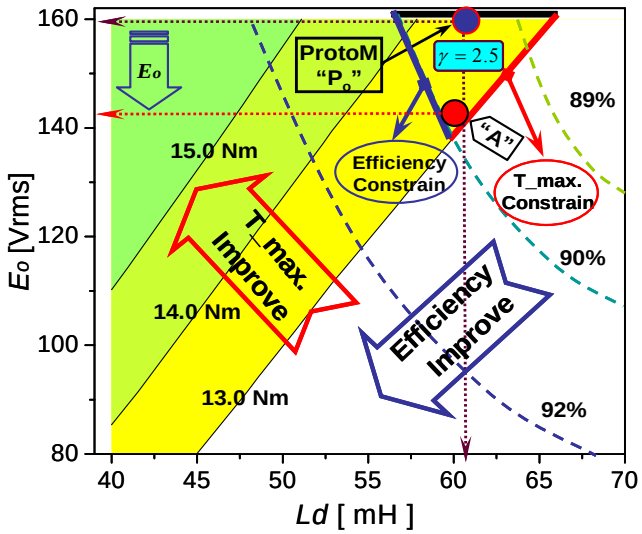

Fig. 10. Torque-Efficiency map analysis based on prototype LSPMM "P_o"

C. *Torque-Efficiency Map Analysis*

In this paper, the reduction of PM material in a double-layer LSPMM design is studied with given torque and efficiency constrains, which is determined as comparing with its original IM, that maintaining maximum output torque capability and improving efficiency 3%, as TABLE I lists.

Based on the single-phase 2000W IM_b model, a double-layer LSPMM design, adopted "M2B" model structure, is introduced as a prototype "P_o" model, which basically satisfied above torque and efficiency constrains that proved by test. By using presented equivalent circuit method, the LSPMM "P_o" generates maximum output torque ($T\_max.$) close to 13.0Nm and efficiency at steady state (η) almost 90%, which are used as predetermined constrains in the simulation of magnet reduction design.

In this study, for giving guidance in the high saliency rotor structure design with given torque and efficiency constrains, an efficient method, "torque-efficiency map" by performing steady state equivalent circuit simulation is proposed. Fig. 10 illustrates the map based on the prototype LSPMM "P_o" model. The torque and efficiency characteristics are mapped as the functions of significant machine characteristics, such as back-EMF (E_o) reacted in main windings at 3000rpm synchronous operation and d-axis inductance L_d, with rotor saliency ratio γ=2.5 defined as ($\gamma=L_q/L_d$).

It is found that the improvement of torque and efficiency along different designs directions, that the larger E_o helps to increase $T\_max.$, but against to efficiency improvement. On the other hand, the lower d-axis inductance generally benefits to both torque and efficiency performance.

In the (γ=2.5) map, the torque curves crossing with the efficiency curves, and the superposition region enclosed region, is obviously satisfies the desired torque and efficiency constrains, such as the marked point "P_o" insider the torque curve of 13.0Nm and efficiency curve of 90% region, that suggests the prototype LSPMM works at rated operation, and

corresponds to back-EMF and L_d [160V_{rms}, 61.5mH].

This torque-efficiency map method is connected with magnet usage estimation based on the judgment of E_o generally proportional to the magnet usage. In inverse, the decreased of E_o is used to estimate the reduction of magnet usage in high rotor saliency LSPMM design [9].

Therefore, the point "P_o" posited in the enclosed region indicates that the prototype LSPMM is not the fittest design from minimum magnet standpoint. Since "P_o" corresponding to a higher E_o value about [160V_{rms}] in the design region, a developed design point "A" at crossing point that critically satisfying torque and efficiency constrains, corresponding to lower E_o value about [142V_{rms}]. It is thought to be the fittest design point. Due to the approximate 10% decreasing of E_o, the improve design from "P_o" to "A" is estimated to save about 10% amount of PM in prototype LSPMM.

Further, with considering the higher rotor saliency ratio γ {3.0; 3.5; 4.0}, the torque-efficiency map is made under the same simulation ranges of E_0 and L_d, as Fig. 11 shows. It is found that the enclosed superposition region of the torque and efficiency constrains are enlarged gradually.

As the design point "A" determination, the minimum magnet design points are determined in each enclosed design region, and the further reduction of magnet is estimated. The design point "B", corresponding to about [120V_{rms}, 55.0mH] in region of (γ=3.0), by which 25% magnet reduction is estimated. And the design point "C", corresponding to nearly [105V_{rms}, 52.0mH] in region of (γ=3.5), and 35% magnet reduction is estimated. The higher rotor saliency benefits to magnet reduction in LSPMM with given performance constrains is confirmed.

Then, according to the above torque-efficiency map analysis, the prototype LSPMM "P_o" model is rebuilt using the estimated reduced amount of PM material. The corresponding predicted back-EMF and *d-q* axis inductance characteristics are achieved by optimizing the double-layer IPM rotor geometry.

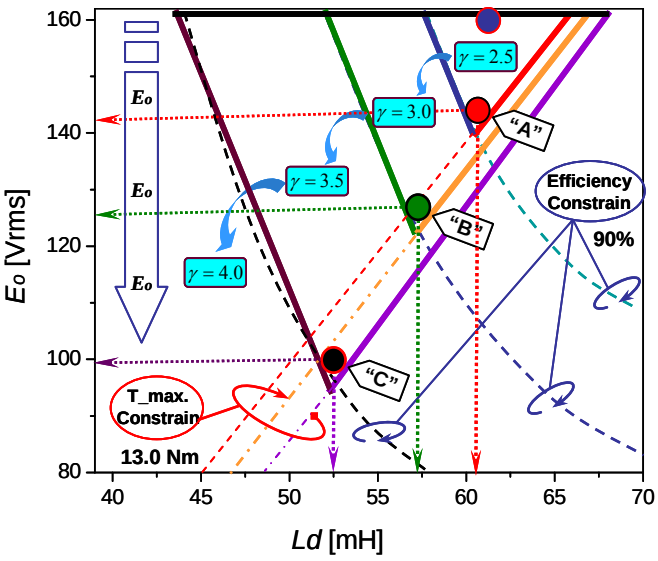

Fig. 11. Developed Torque-Efficiency map for magnet reduction analysis

IV. High Rotor Saliency Double-Layer Rotor Design

The higher rotor saliency design for realizing magnet reduction in LSPMM is presented in this section. Base on the prototype LSPMM "P_o" model, the double-layer IPM rotor structure is rebuilt by optimizing the buried PM segments, and air-gap fields. The design variables of double-layer IPM rotor structure, and the margining limits for mechanical strength consideration, are given in Fig. 12.

The prototype LSPMM "P_o" model is standard as 100% amount of PM, and design "A" model with 90% amount, design "B" model with 75% amount, and design "C" model with 65% amount, respectively. The dimensions of gradually reduced magnet as estimated are visualized in Fig. 13.

Similar to the prototype LSPMM "P_o" model, the thickness of PM segments is fixed at 2.6mm, and the slope angle of side PM segment α is still 20°. The buried air-gap regions are enlarged for decreasing the *d*-axis inductance, and the gap between PM layers are increased for increasing the *q*-axis inductance, both of which benefits to improve rotor saliency, further to increase reluctance torque generation. In the model design, the objectives of phase back-EMF and *d-q* axis inductance with rotor saliency predicted by the torque-efficiency map analysis are achieved.

The shape of redesigned LSPMM models "A" and "B" comparing with model "P_o", are illustrates in Fig. 14. In conclude, both of the LSPMM "A" and "B" achieved the torque and efficiency constrains of "P_o" model standard according to equivalent circuit analysis. But, the model "C", since too much PM reduced, can not achieve the rotor saliency 3.5 by optimizing double-layer IPM rotor structure to satisfy the constrains. TABLE III lists the characteristics comparison of each model in magnet reduction design.

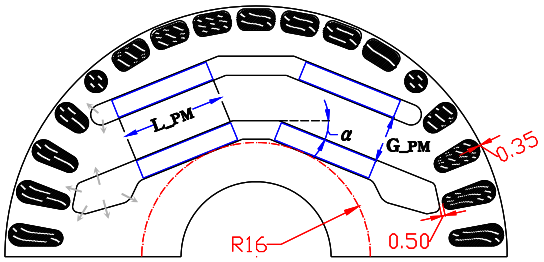

Fig. 12. Double-layer IPM rotor design based on IM_b model

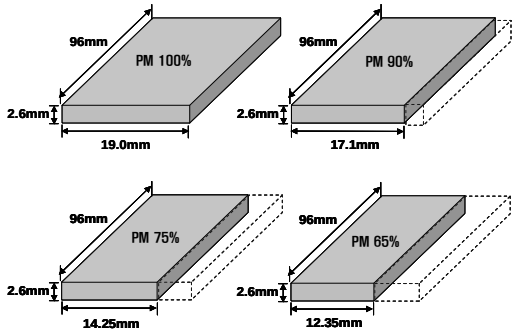

Fig. 13. Dimensions of reduced PM segments in double-layer IPM design

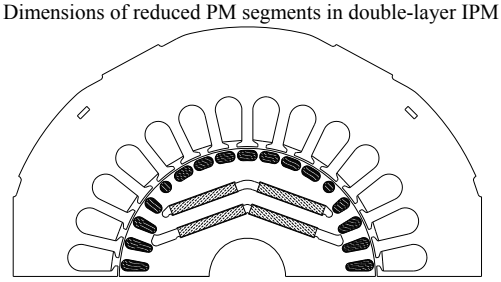

(a) Prototype LSPMM "P_o"[100% PM]: (G_o_PM=3.9mm)

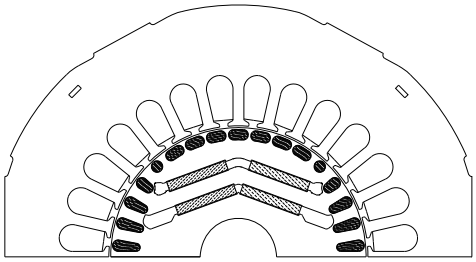

(b) Optimized LSPMM "A" [90% PM]: (G_o_PM=4.3mm)

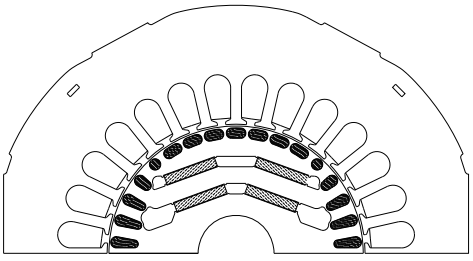

(c) Optimized LSPMM "B" [75% PM]: (G_o_PM=5.4mm)

Fig. 14. Magnet reduction design of double-layer IPM LSPMM models

TABLE III
PERFORMANCE COMPARSION IN MAGNET REDUCTION DESIGN

Model	IM	M_"P_o"	M_"A"	M_"B"	M_"C"
PM use [%]	0	100	90	75	65
Back-EMF[V_{rms}]	0	160	141.3	123.1	101.5
Rotor Saliency	-	2.5	2.5	3.0	3.2
T_Ave.[Nm]	6.5	6.5	6.5	6.5	6.5
T_Max.[Nm]	13.2	13.2	13.0	13.0	12.5
Efficiency[%]	88.0	90.8	91.0	91.0	90.0
Cost of Material	100	188	179	166	157
PM : Cost [%]	0	47	44	40	36

V. Results And Discusses

The validity of presented torque and efficiency performance analysis in LSPMM design is confirmed by experiment method. The redesigned LSPMM model "B" with saving 25% amount of PM reduction is manufactured, and the starting torque, maximum output torque capability and efficiency performance at rated operation are tested. Fig. 15 shows the fabricated LSPMM "B" and experiment setup.

For verifying the presented IPM rotor structure advantage in torque and efficiency improvement benefits to magnet reduction, the concerned performance of LSPMM "B" are compare with the prototype LSPMM "P_o" and base IM_b.

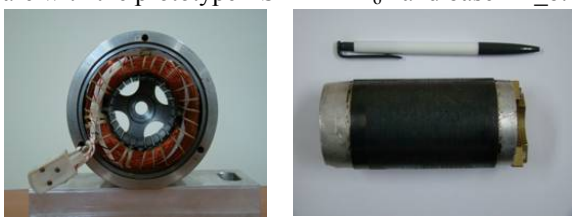

(a) Stator and rotor configuration of LSPMM

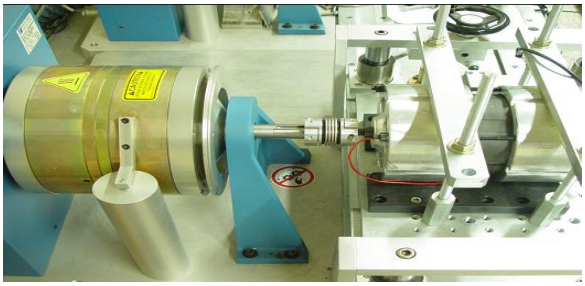

(b) Testing apparatus for motor performance measurement

Fig. 15. Fabricated LSPMM and experiment setup

A. Torque Characteristic at Start-up Operation

The asynchronous starting torque of IM_b during start-up operation is tested with connecting starting capacitor 25μF and running capacitor 30μF. As Fig. 16(a) shows, the starting torque increases from 1.8Nm at beginning to 6.0Nm at peak.

On the other hand, based on the stator electric circuit simulation analysis, the larger starting capacitor 35μF and running capacitor 60μF are employed in the LSPMM "B" start-up operation, which helps to overcome magnet braking torque and improve starting torque. The validity of equivalent circuit method for starting torque characteristic analysis is confirmed by LSPMM "B" test result, as Fig. 16(b) shows,

that both 3.0Nm at starting moment and 6.5Nm at peak point shows a good agreement.

B. Machine Performances at Steady State

From the steady state equivalent circuit analysis, the LSPMM "B" with 25% reduction of PM usage, realized 3% improvement of efficiency at rated 3000rpm operation while maintaining maximum output torque capability comparing with the base IM_b.

The maximum output torque of LSPMM "B" is confirmed by 2D FEA, that the average value 13.2Nm is a little higher contract to the 13.0Nm calculated by equivalent circuit method. It is similar to the asynchronous induction torque 13.3Nm of IM_b by test. And, the LSPMM "B" performances is tested and compared with IM_b (test temperature 25°C by fan-cooling), as Fig. 17 illustrates. It is observed from Fig. 18 that the calculated efficiency results are higher than their corresponding tested results, which is thought caused by only fundamental component of back-EMF is considered in equivalent circuit analysis. Since similar proportional enlarged between the calculated result and test data, the predicted 3% improvement of efficiency by developing IM_b to be LSPMM is well proved.

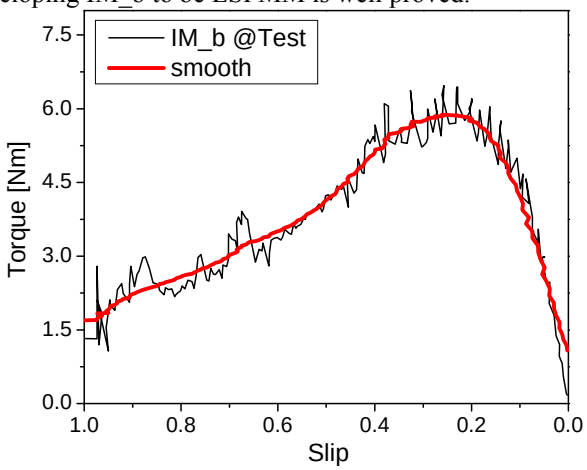

(a) Starting torque of IM_b by test

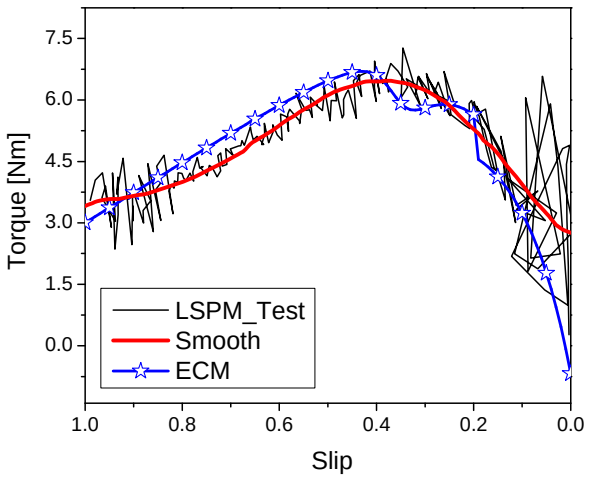

(b) Starting torque of LSPMM "B" by test and ECM

Fig. 16. Asynchronous starting torque results comparison

In final, the tested main performances of the base IM_b, prototype LSPMM "P_o" and redesigned LSPMM "B", are compared, as Fig. 19 shows. The almost same machine performances are achieved in the presented magnet reduction design is verified.

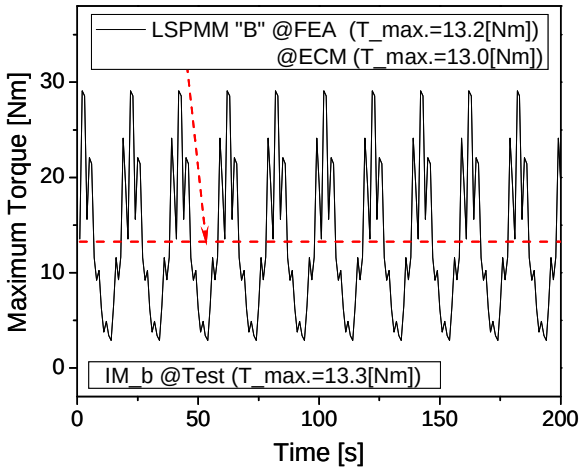

Fig. 17. Maximum output torque of LSPMM "B" at synchronous operation

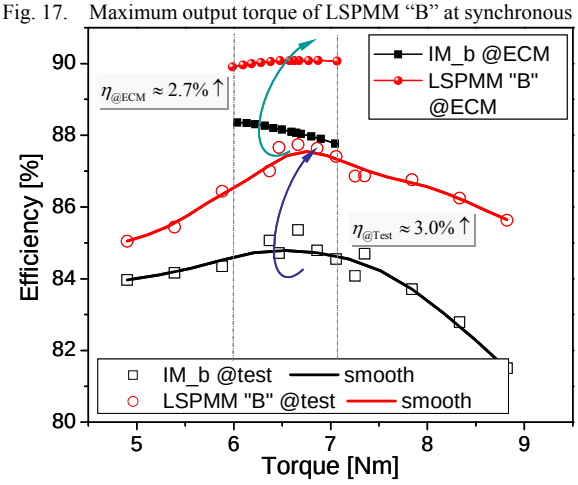

Fig. 18. Efficiency comparison between IM_b and LSPMM "B"

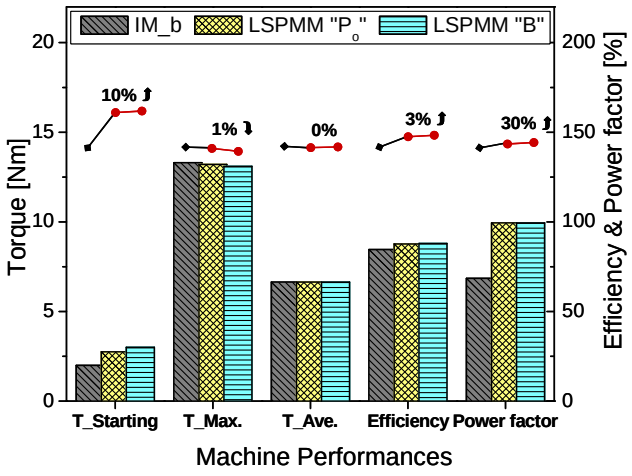

Fig. 19. Performances comparison between IM_b, LSPMM "P_o" and "B"

CONCLUSION

This paper presented a theoretical and experimental study of cost reduction in a single-phase LSPMM by emphasizing structure advantage of IPM rotor to lower the dependency on PM usage in IPM machine. By creating high rotor saliency, the hybrid balance of reluctance torque to magnet torque is enhanced, which helps to promote the decreased machine performances since PM reduction.

The proposed torque-efficiency maps are well applied for guiding double-layer IPM rotor designs with satisfying given torque and efficiency constrains. And the estimated PM reduction is realized with predicted machine characteristics as well as higher rotor saliency. The LSPMM performance prediction by using presented equivalent circuit method coupled with 2D FEA are validated by acceptable test results.

In practice, the rotor structure design for cost reduction should satisfy the mechanical strength requirement. And the tradeoff of PM material cost and manufacture difficulties are usually to be considered.

REFERENCES

[1] Timothy J. E. Miller, "Single-Phase Permanent-Magnet Motor Analysis", *IEEE Trans. On Indus. Appl., Vol. IA-21, No. 4, May/June 1985*.

[2] Nicole Bianchi, Thomas M. Jahns, “Design, Analysis, and Control of Interior PM synchronous Machines”, *IEEE-IAS* Electrical Machines Committee.

[3] Timothy J. E. Miller, "Line-start Permanent-Magnet Single-phase Steady-State Performance Analysis", *IEEE Trans. On Indus. Appl., Vol.40. No. 2, March/April 2004.*

[4] Mircea Popescu, Timothy J. E. Miller, Malcolm McGilp, Giovanni Strappazzon, Nicolla Trivillin, Roberto Santarossa, "Asynchronous Performance Analysis of a Single-Phase Capacitor-Start, Capacitor-Run Permanent Magnet Motor”, *IEEE Trans. On Energy Conversion, Vol.20. No. 1, March 2005.*

[5] Jie Zhou, and King-Jet Tseng, "Performance Analysis of Single-Phase Line-Start Permanent-Magnet Synchronous Motor," *IEEE Trans. On Energy Conversion, Vol. 17, No. 4, December 2002.*

[6] G. H. Kang, B.K. Lee, H. Nam, J. Hur, and J. P. Hong, “Analysis of Single-Phase Line-Start Permanent-Magnet Motors Considering Iron Loss and Parameter Variation With Load Angle,” *IEEE Trans. On Indus. Appl., Vol. 40, No. 3, May/June 2004.*

[7] Ji-Yong Lee, Sang-Ho Lee, Geun-Ho Lee, Jung-Pyo Hong, Jin Hur, “Determination of Parameters Considering Magnetic Nonlinearity in an Interior Permanent Magnet Synchronous Motor,” *IEEE Transaction on Magnetics,* vol. 402, no. 4, April 2006.

[8] John M. Miller, *Propulsion systems for hybrid vehicles*, The Institution of Electrical Engineers, 2004. pp. 168-170

[9] Liang Fang, Jae-woo Jung, Jung-Pyo Hong, and Jung-Ho Lee, “Study on High-Efficiency Performance in Interior Permanent-Magnet Synchronous Motor With Double-Layer PM Design,” *IEEE Trans. Magn., vol.44, no.11, November 2008*